EFFECTS OF THE INFLOW OF OUTDOOR AIR THROUGH A BREATHING WALL ON THERMAL INSULATION PROPERTIES AND INDOOR CLIMATE IN WINTER

Seonghwan Yoon*, Akira Hoyano* and Kazumasa Gonaikawa**
*Tokyo Institute of Technology, Yokohama, Kanagawa, 226-8502, Japan
**Higashi Nihon House Co. Ltd. Morioka, Iwate, 220-0062
fax: +81-45-924-5553
e-mail: syun@hy.depe.titech.ac.jp

ABASTRACT Breathing walls were installed on opposite sides of a scale mock-up model of a housing structure that was situated in an artificial climate test room. We analyzed the thermal insulation capability, heat recovery effect and indoor climate for the inflow of outdoor air across the breathing wall. The rate of heat recovery reached 30% under strong winds of up to 8 m/s. Even when the ventilation rate tripled due to the strong wind, the temperature difference in the vertical direction was less than 2 K.

1 Introduction

Recent demands by the Japanese public for more energy efficient housing have typically been met by the housing industry by making housing more airtight and adding high-thermal insulation. However, in temperate and humid climate regions, such as the Kanto region in Japan, the utilization of natural ventilation at wall surfaces may be a more efficient approach. Such systems require no mechanical ventilation equipment and yet allow the building's thermal insulation capability to be fully exploited, without the internal condensation that is normally associated with an energy efficient, well-sealed house.

With this in mind, we developed the "Breathing Wall"[1], an architectural element and key component of our proposed natural ventilation system. In previous studies, the effects on thermal insulation capacity of pressure differences across the breathing wall and the occurrence of internal condensation within the breathing wall were evaluated experimentally for a steady state[2]. The breathing wall is constructed of aluminum sheets that are installed in a wood panel frame, forming a multiple air-layered architectural Element. Each layer has several finely-spaced circular perforations. As the outdoor wind pressure and air temperature change, inflow and outflow occur across the breathing wall. Heat and moisture transfer also occur, thus allowing the wall to breath under natural climatic conditions.

In the present study, breathing walls were installed on opposite sides of a scale mock-up model of a housing structure that was situated in an artificial climate test room. We quantitatively analyzed the thermal insulation capability, heat recovery effect and indoor climate for the inflow of cold outdoor air across the breathing wall. The effects of wind velocity were simulated by varying the wind pressure differential across the breathing wall under indoor and outdoor air temperatures of 25°C and 5°C, respectively.

2 Experimental setup

Simulation results of previous studies revealed the most effective hole diameter/spacing for sheet 1 to be 1.0/22.0 mm (opening ratio 0.7%). Sufficient ventilation was found to be provided under these conditions, even if the outdoor wind speed is zero. Moreover, under these conditions, no internal condensation was found to occur even at maximum wind velocity (8 m/s) (the probability of exceeding the maximum velocity is almost 0% in Tokyo).

The internal structure of the breathing wall (1955×450×90 mm), i.e. the area which lies between the inner and outer perforated plywood panels (thickness = 3 mm), consists of alternating layers of 11 perforated PET-Al sheets and 12 paulownia-wood lattice (150×150 mm) core sheets that are arranged to form ten 5-mm-thick air layers (Fig.1). Two breathing walls were installed opposite to each other in a scale mock-up model (3700×1550×2535 mm). All other members in the model were covered with polystyrene boarding to provide good insulation and an air-tight seal between the inner and outer environments (Fig.2).

Fig.3 shows the scale mock-up model in the artificial climate test room (6800×7200×4600 mm). The climate test room was used to automatically maintain outdoor relative humidity and air temperature at the desired values. Experimental test conditions simulated the typical winter climate of Tokyo, i.e. indoor and outdoor air temperatures of 25°C and 5°C, respectively. The effect on the wall of varying wind velocity (3 to 8 m/s) was simulated by varying the pressure difference across the breathing wall from 1.5 to 10.2 Pa (Fig.4). Measurements, corresponding sensors and sensor positions are described in Fig.5.

3 Experimental results

3.1 Internal temperature distribution

Fig.6 shows the internal temperature distribution measured at each aluminum-foil sheet at measuring position B (Fig.5(1)) for a 8 m/s wind velocity (inward flow) and for the steady state condition (no wind). Under the steady state condition, even for an outdoor air temperature of 5°C, the temperature of the air between the inner-most sheets increased by 16.4°C at the lower part of the wall, because air passing through the outdoor surface is preheated via heat exchange between the aluminum-foil sheets and the air layers.

When outdoor air is forced through the wall due to outdoor wind pressure, the temperature gradient between the sheets near the indoor surface increases and that between the sheets near the outdoor surface decreases. Since the largest temperature gradient is found between sheet 1 and air layer 1, maintaining the emission rate of sheet 1 appears to be essential in order to provide good thermal insulation properties for the breathing wall under strong wind conditions (8 m/s). Ten minutes after initiating a continuous 8 m/s wind pressure condition, the internal temperature distribution reached the steady state condition, as indicated by the temperature gradient of less than 1K between sheets 3-11.

3.2 Heat flux of surfaces

Since heat flux provides an indication of the average of thermal insulation property of the breathing wall, we analyzed the thermal insulation property of the breathing wall by measuring the heat flux across the inner surface of the wall at the upwind side. Fig.7 shows the heat flux across the inner surface of the wall at the upwind side for a 3 m/s wind velocity (inward flow), the most frequent wind velocity condition in winter in Tokyo.

The heat flux at the lower part of the wall (measuring position B) was 10 W/m^2 under the no wind condition. The temperature differences between the indoor and outdoor air was 20K, which provides an ACH (Air Change per Hour) of 0.5. These conditions provide sufficient thermal insulation properties when employed in temperate climate regions.

The heat flux at the upper part of the wall (measuring position A) under a wind velocity of 3 m/s occurs in a manner that is temporally similar to that which occurs under the no wind condition and provides sufficient thermal insulation properties for temperate climate regions. The heat flux at the lower part of the wall (measuring position B) increases to 30 W/m^2. The heat flux at the lower part of the wall includes 12.4 W/m^2 of heat loss due to infiltration. If this heat loss is excluded, the heat flux at the lower part of the wall is very similar to the heat flux under the no wind condition.

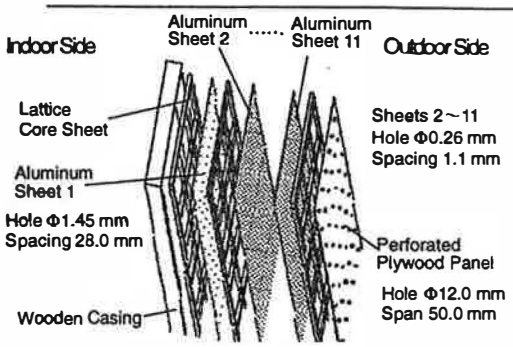

Fig.1 Breathing wall structure

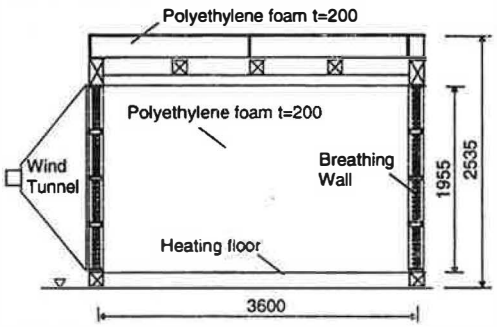

Fig.2 Cross-section of the scale mock-up

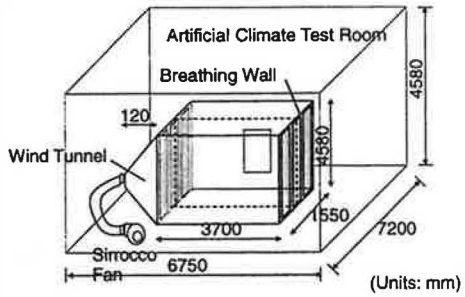

Fig.3 Scale model in the artificial climate test room

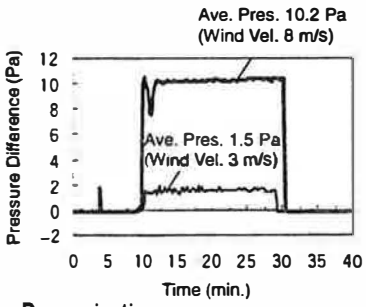

Fig.4 Pressurisation progress

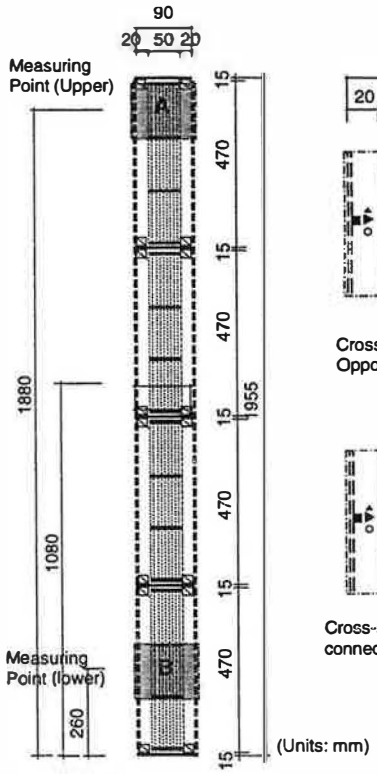

(1) Breathing Wall Cross-section

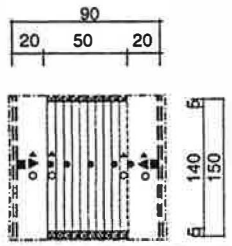

Cross-section of the Wall Opposite to Wind Tunnel

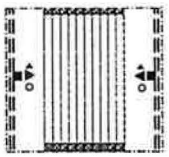

Cross-section of the Wall connected to the wind tunnel

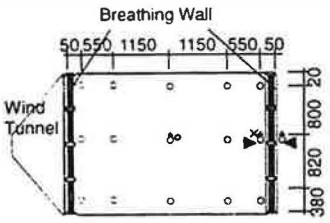

Scale Mock-up Model

(Units: mm)

●: Surface temperature (T-CC Thermal Couple)
○: Air temperature (T-CC Thermal Couple)
▲: Relative humidity (High Polymer Capacity Type)
■: Heat Flux of Surface (80×80 mm)
⋈ Pressure difference (Differential Transducer)
X: Airflow Velocity (Ultrasonic Anemometer)

(2) Sensors and sensor positions

Fig.5 Sensors and sensor positions

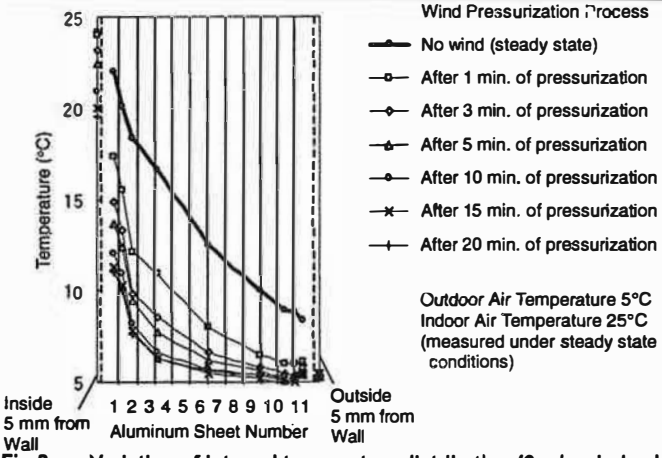

Fig.6 Variation of internal temperature distribution (8 m/s wind velocity)

3.3 Heat recovery effect

When outdoor air flowed inward across the breathing wall, heat exchange occurred between the surface of the perforated aluminum sheet and the air layers. The heat loss due to ventilation was expected to be lower due to the effect of heat recovery. The rate of heat recovery and its magnitude, due to the change in wind pressure corresponding to the change in wind velocity from 0 m/s to 3 m/s or 8 m/s, were calculated and are shown in Fig.8. The following equations were used to calculate these values:

$$\eta=(I_o - I_{inflow})/(I_o-I_{outflow}) \quad (1)$$

$$Q_{hr} = \rho V(I_o-I_{inflow}) \quad (2)$$

Where: η - *heat recovery rate (%)*
I_o - *the enthalpy of outdoor air (J/kg)*
$I_{outflow}$ - *the enthalpy of outflow air (J/kg)*
V - *the quantity of ventilation (m^3/m^2s)*
Q_{hr} - *amount of heat recovery (W/m^2)*
I_{inflow} - *the enthalpy of inflow air (J/kg)*
ρ - *air density (kg/m^3)*

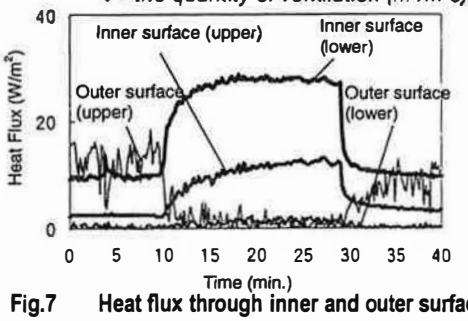

Fig.7 Heat flux through inner and outer surfaces (3 m/s wind velocity)

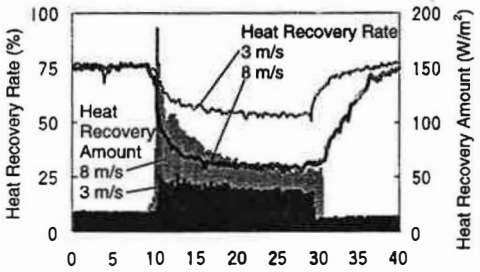

Fig.8 Variation in heat recovery rate in % and in W/m²

The magnitude of heat recovery reached 40 W/m^2, for wind pressure equivalent to a 3 m/s wind. Of this amount, heat recovery was 30 W/m^2. Given an adequate air flow, heat recovery is higher than heat loss due to ventilation and thus little energy is consumed even though continual indoor ventilation is provided under natural conditions. Thus, the rate of heat recovery was 55%, and reached 30% under a strong wind of 8 m/s.

3.4. Distribution of indoor air temperature

The effect of infiltration on the indoor climate was investigated by analyzing the distribution of the indoor air temperature under the strong wind condition (8 m/s) in winter. The results are shown in Fig.9 after 20 minutes of strong wind (8 m/s). The temperature distribution was drawn based on interpolation of actual air temperature data measured at 15 points (Fig.5).

When the ventilation rate tripled due to the strong wind, the air temperature in the area 50 cm from the outer surface of the wall on the upwind side was 5K lower than that under the no wind condition. The temperature difference in the vertical direction, however, was less than 2K. Thus, no adverse effects on residents are believed to be associated with the use of the breathing wall.

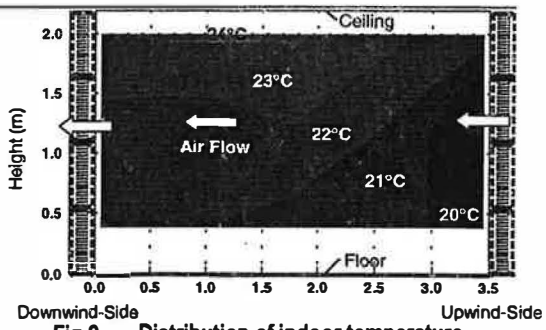

Fig.9 Distribution of indoor temperature 8 m/s after air change tripled

In the present experiment, the air speed along the inner surface of the breathing wall was measured to be lower than 0.05 m/s; therefore, the present experiment can be considered as having been performed under a near-static conditions. Despite the cold air that passes through the wall under the relatively strong wind condition, cold drafts are not expected to occur within the interior because the actual indoor air velocity is maintained below approximately 0.2 m/s and mixing occurs with the naturally rising warm indoor air (natural convection). However, confirmation of this assumption requires further analysis.

4 Conclusions

We quantitatively analyzed the effects of the inflow of outdoor air across a breathing wall on thermal insulation properties and indoor climate in winter. The rate of heat recovery reached 30% under strong winds of up to 8m/s. In addition, even when the ventilation rate tripled due to the strong wind of 8 m/s, the temperature difference in the vertical direction was less than 2K.

5 References

Akira Hoyano et al. (1995): Proposal of a Breathing Wall as an Architectural Member for a Passive Solar System in a Temperate and Humid Climate Region. *Proceedings of Pan Pacific Symposium on Building and Urban Environment Conditioning in Asia*, March 16-18, Nagoya, JAPAN, Vol. 1, pp. 43-52

Seonghwan Yoon and Akira Hoyano (1998): Passive Ventilation System that Incorporates a Pitched Roof Constructed of Breathing Walls for Use in a Passive Solar House, *Solar Energy*, Journal of the International Solar Energy Society, Vol. 64/Issue 4-6, pp. 189-195

Acknowledgements

Primary support for this research was granted by the National Science Foundation of the Ministry of Education (Grant No. 09650645). Sincere gratitude is extended to TDK Co. Ltd., for kindly providing the sensors for measuring relative humidity.